

# Antisense Expression of a Cell Wall–Associated Protein Kinase, WAK4, Inhibits Cell Elongation and Alters Morphology

David Lally,<sup>1</sup> Peter Ingmire,<sup>1</sup> Hong-Yun Tong, and Zheng-Hui He<sup>2</sup>

Department of Biology, San Francisco State University, 1600 Holloway Avenue, San Francisco, California 94132

**The Arabidopsis cell wall–associated receptor-like kinase (WAK) gene family contains five highly related members whose products are suited for exchanging signals between the intracellular and extracellular compartments. WAK members are expressed in specific organs and regulated differentially by various biotic and abiotic factors. To gain further insight into how WAKs function during development, we used a glucocorticoid-inducible system to express ectopically the WAK4 antisense gene. The induced expression of the WAK4 antisense gene resulted in a significant decrease of WAK proteins. Ninety-six hours after the induction of WAK4 antisense expression, WAK proteins became undetectable. Cell elongation was impaired, and lateral root development was blocked. The level of WAK protein could be controlled by the concentration of the applied inducer, dexamethasone, and was correlated with the severity of the cell elongation inhibition phenotype. These results suggest that the WAKs serve a vital role in cell elongation and are required for plant development.**

## INTRODUCTION

The plant cell wall is composed of a complex network of cellulose microfibrils, polysaccharides, and glycoproteins (Carpita and Gibeaut, 1993). Cell wall components are made and secreted by their enclosed or adjacent cells and in return define the cell's immediate environment and shape. It is proposed that components of the cell wall interact with the plasma membrane and the cytoplasm and that those interconnections are pivotal in influencing cell shape, cell size, cell differentiation, and cell death (Carpita et al., 1996; Braam, 1999; Cosgrove, 1999; Kohorn, 2000). The cell wall not only defines the structural and morphological identity of the plant cell but also mediates how plant cells interact with each other to maintain organismal integrity and interact with the environment to survive (Cosgrove, 1999).

The cell wall contains numerous potential signaling molecules, including small peptides, proteins, and oligosaccharides, which may interact with receptor molecules on the cell surface to elicit cellular responses (McCarty and Chory, 2000; Torii, 2000). The connectivity of the cell wall components also plays an important role in growth and development. The relaxation of the cell wall can have a direct and profound effect on plant morphogenesis (Fleming et al., 1997). Changes of cell wall architecture are sensed through direct physical links between the cell wall and the plasma membrane, and these links have been proposed to play im-

portant roles in plant cell communication and plant development. Together with the cytoskeletal network and the plasma membrane, the cell wall forms a molecular continuum that is thought to be essential in determining the direction of cell expansion and, ultimately, the cell's final shape (Wyatt and Carpita, 1993; Baskin et al., 1994; Roberts, 1994; Wymer and Lloyd, 1996; Kohorn, 2000). Studies have visually detected direct physical links between the cell wall and the cytoplasm (Pont-Lezica et al., 1993; Zhu et al., 1993). Nevertheless, the nature of the molecular connections between the cell wall and the cytoplasm is not very clear, and exactly how the molecular continuum functions in cell expansion is largely unknown.

A family of cell wall–associated receptor-like kinases (WAKs) has been identified in Arabidopsis. WAKs are plasma membrane proteins with serine/threonine kinase domains in the cytosol and extracellular domains tightly associated with the cell wall (He et al., 1998, 1999). The extracellular domains of WAKs contain several repeats homologous with vertebrate epidermal growth factor, a motif found in many proteins involved in extracellular interactions (Appella et al., 1987; Rebay et al., 1991; Stenberg et al., 1999). WAKs are suitable candidates for directly linking the extracellular and intracellular compartments. Different WAK members are expressed in specific organs and respond to various biotic and abiotic stimuli (He et al., 1998, 1999). The expression of WAK1 is upregulated during pathogen response. This upregulation of WAK1 is required for Arabidopsis plants to survive during the pathogen response, indicating that WAK1 may be involved in pathogenesis (He

<sup>1</sup> These authors contributed equally to this work.

<sup>2</sup> To whom correspondence should be addressed. E-mail zhe@sfsu.edu; fax 415-338-2295.

et al., 1998). Different WAKs have divergent structures in their extracellular domains, which are N-terminal to the epidermal growth factor-like repeats, suggesting that they may interact with different ligands in the cell wall (He et al., 1999). To gain further insight into how WAKs function during plant development, we used the glucocorticoid-inducible system to control the antisense expression of WAK4. We report here that induced WAK4 antisense expression reduced levels of WAK protein. The induction of WAK4 antisense expression correlates with the WAK protein decrease and the developmental arrest. Our results suggest that WAKs are involved in cell elongation and are required for Arabidopsis development.

## RESULTS

### WAK4 Antisense Expression Resulted in WAK Suppression

To better understand the functional role of WAK4, we used the glucocorticoid-inducible system (Aoyama and Chua, 1997) to control the expression of a WAK4 antisense gene. The system has been used successfully to analyze gene functions (McNellis et al., 1998; Kim et al., 1999; Yoshizumi et al., 1999). In the inducible system, the expression of transgenes can be tightly controlled by exogenous application of dexamethasone (DEX), a synthetic glucocorticoid steroid (Aoyama and Chua, 1997). Specifically, the full-length WAK4 genomic fragment was cloned into the pTA7002 plasmid in a reverse orientation behind the 6XUAS GAL4-inducible promoter. This construct was transformed into Arabidopsis wild-type plants (ecotype Columbia) by using a vacuum infiltration-based method (Bechtold et al., 1993). True transformants were selected on Murashige and Skoog (1962) (MS) medium containing hygromycin. From 23 independent transgenic lines, seven lines showed strong consistent phenotypes when DEX was applied, and they were selected for further analysis. T4 seedlings homozygous for the WAK4 antisense gene (W4A) were used for the studies described here. Unless specified otherwise, the results presented here are derived from studies of one (W4A-4) of the seven W4A transgenic lines analyzed. There is no observable defect or lethality in W4A lines when the expression of the antisense transgene is not induced. As controls, transgenic plants carrying the pTA7002 empty vector or the  $\beta$ -glucuronidase (*GUS*) gene were generated. Control experiments were performed with wild-type plants, and the results were confirmed with control transgenic plants.

RNA gel blot analyses were used to investigate the effect of ectopic WAK4 antisense expression on steady state levels of the endogenous WAK4 mRNA. Wild-type and W4A plants were sprayed with either 30  $\mu$ M DEX or a mock solution. At various times after spraying, leaf tissue was col-

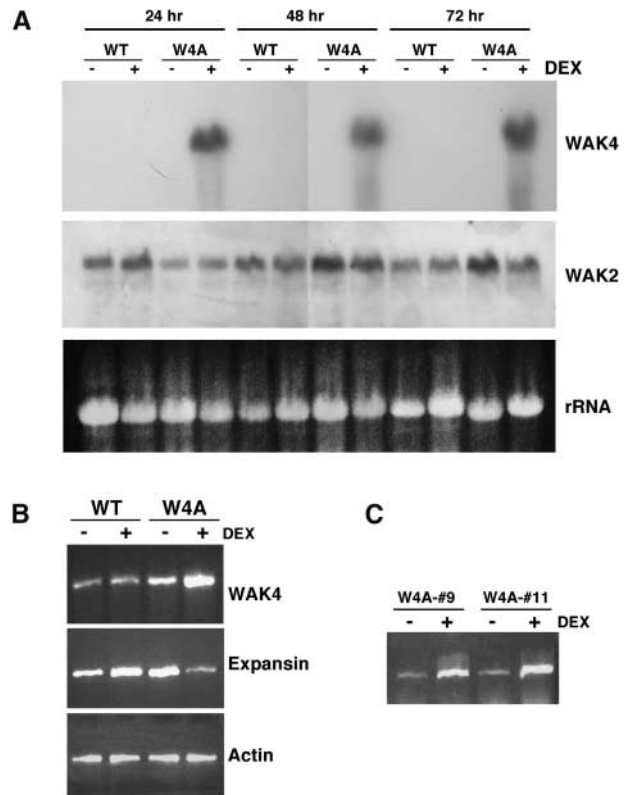


**Figure 1.** Induced WAK4 Antisense Expression Affects WAK4 Transcript Accumulation.

**(A)** RNA gel blot analysis of WAK4 antisense transgenic plants. Wild-type (WT) and WAK4 antisense transgenic (W4A) plants (10-leaf stage) were sprayed with either a mock solution (–) or 30  $\mu$ M DEX (+). At various times (24, 48, and 72 hr) after the treatments, leaf tissues were collected for RNA extraction. Fifteen micrograms of total RNA was fractionated and blotted onto nylon membranes for analysis. Duplicated RNA gel blots were probed with gene-specific probes (WAK2 and WAK4). As a control for equal loading, ethidium bromide staining of 28S rRNA is shown at the bottom (rRNA).

**(B)** RT-PCR analysis of WAK4 and expansin expression in DEX-induced W4A plants. Wild-type and WAK4 antisense (W4A) plants were sprayed with a mock solution (–) or 30  $\mu$ M DEX (+). Twenty-four hours after the spraying, leaf tissues were harvested and used for RNA isolation. Equal amounts of RNA from each sample were used for RT-PCR analysis of either WAK4 or expansin expression. The levels of actin were assayed as controls.

**(C)** RT-PCR analysis of WAK4 expression in two other DEX-treated W4A lines. WAK4 antisense (W4A-#9 and W4A-#11) plants were sprayed with a mock solution (–) or 30  $\mu$ M DEX (+). Twenty-four hours after the spraying, leaf tissues were harvested and used for RNA isolation. Equal amounts of RNA from each sample were used for RT-PCR analysis of WAK4 expression.

lected for total RNA extraction. A specific WAK4 probe (see Methods) was used to detect WAK4 transcripts. Figure 1A shows that surprisingly, DEX led to an increase of WAK4 transcripts in W4A plants. Twenty-four hours after DEX treatment, there was a significant increase of the endogenous WAK4 transcripts in W4A plants (Figure 1A). DEX did not have any effect on WAK4 expression in wild-type plants. To confirm that the increased signal was the result of WAK4 transcript accumulation, reverse transcription–polymerase chain reaction (RT-PCR) analysis using WAK4 gene-specific primers was performed on isolated RNA samples (Figure 1B). WAK4 transcripts increased 24 hr after DEX application (Figure 1B), which is consistent with the RNA gel blot analysis result. This increase was observed in all W4A lines analyzed, including W4A-9 and W4A-11 (Figure 1C). To verify RT-PCR specificity for WAK4, we subcloned the RT-PCR product shown in Figure 1B into a PCR cloning vector and sequenced it. Sequence information confirmed that the RT-PCR product carried the expected WAK4 gene fragment (data not shown).

WAK4 transcripts were not detectable in leaf tissue by RNA gel blot analysis (Figure 1A), which is consistent with previous data (He et al., 1999). However, using RT-PCR, a more sensitive method, we found that WAK4 was expressed in all organs tested (data not shown), including leaves (Figure 1B). The mRNA levels for WAK2 (Figure 1A) and other WAK members (data not shown) were not affected by W4A expression. For RT-PCR analysis, the expression profiles of actin (as a control) and expansin were included (Figure 1B). Like WAK genes, expansin genes also encode cell wall-associated proteins (Cosgrove, 1997). RT-PCR analysis showed an even level of actin expression in either DEX-treated or untreated wild-type and W4A plants (Figure 2B). It is interesting that DEX caused a substantial decrease of expansin mRNA in W4A plants (Figure 1B), suggesting that the induced WAK4 antisense expression may interact with or influence expansin. How the ectopic WAK4 antisense expression leads to an increase of endogenous WAK4 mRNA is not known. Trace levels of WAK4 antisense RNA also were detected by RNA gel blot analysis in DEX-treated W4A plants (data not shown).

We then tested the effect of DEX treatment on WAK gene expression at the protein level. Total leaf protein was extracted from either DEX-treated or untreated W4A plants, and protein gel blot analysis was performed using a polyclonal antibody raised against the WAK1 kinase domain (He et al., 1996). Given that five WAK members share >86% amino acid identity in their kinase domains and that their predicted full-length sizes are nearly identical (He et al., 1999), the antibody is expected to react with all five proteins (He et al., 1999). The antibody does react to bacterially expressed WAKs (Z.-H. He, unpublished data). WAKs are known to be tightly associated with the cell wall; extraction requires boiling in SDS-DTT (He et al., 1996). Proteins were extracted in the boiling SDS-DTT buffer, and equal samples were run on the gel, blotted to nitrocellulose membranes,

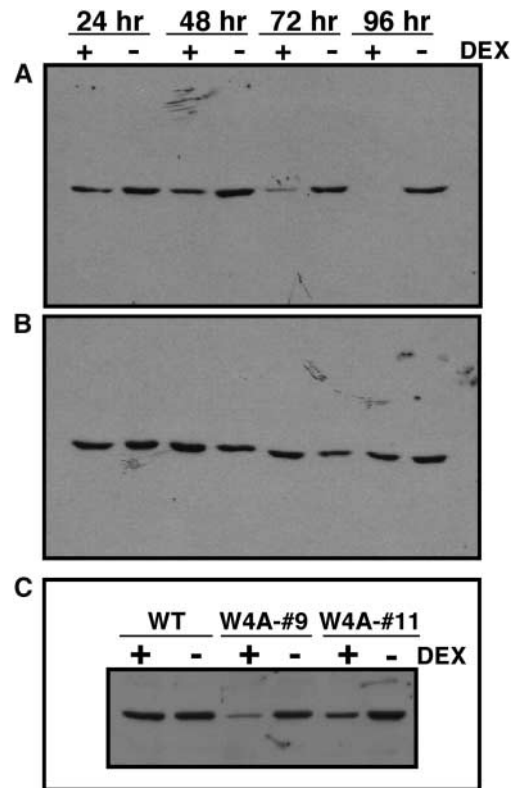


**Figure 2.** Reduced Levels of WAK Proteins by W4A Expression.

**(A)** Protein gel blot analysis with WAK antibody of proteins extracted from WAK4 antisense transgenic (W4A) plants that were sprayed with either a mock solution (–) or 30  $\mu$ M DEX (+) for 24, 48, 72, or 96 hr.

**(B)** Protein gel blot analysis of proteins extracted from wild-type plants that were sprayed as described in **(A)**.

**(C)** Protein gel blot analysis with WAK antibody of proteins extracted from wild-type (WT) and two other transgenic W4A plants (W4A-#9 and W4A-#11) that were sprayed as described in **(A)**. Protein samples were obtained 24 hr after spraying.

and probed with the WAK antibody. Figure 2A shows a noticeable decrease of WAK protein at 24 hr after DEX induction. WAK protein levels continued to decrease until they were undetectable 96 hr after DEX application (Figure 2A). This decrease of WAK protein by DEX treatment was observed in all W4A lines analyzed, including W4A-9 and W4A-11 (Figure 2C). DEX-induced WAK protein reduction in W4A plants was further confirmed by immunocytochemical analysis (see below). DEX treatments have little effect on WAK protein levels in either wild-type plants (Figure 2B) or transgenic empty-vector plants (data not shown). These results indicate that the treatment with DEX dramatically decreased all detectable WAK protein.

### WAK4 Antisense Expression Causes Early Developmental Arrest

DEX dramatically reduced WAK proteins, as indicated by the protein gel blot results. There is a possibility that the

WAK protein reduction in the protein gel blot analysis might be the result of changes in protein extractability. For example, the DEX treatment could cause WAK proteins to be cross-linked to insoluble components of the cell. To address this issue, seed of wild-type and W4A plants were sterilized,

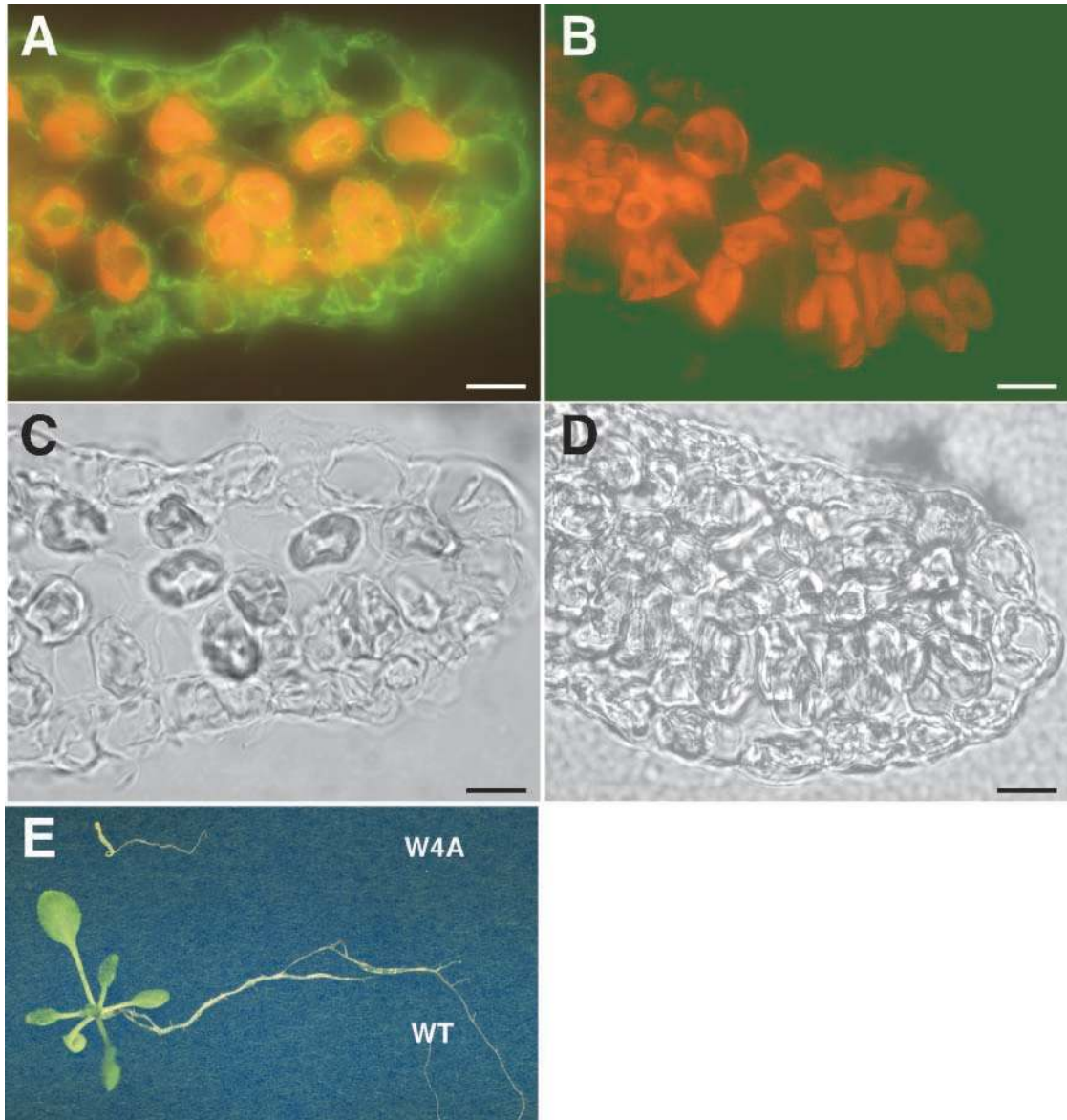


**Figure 3.** Effects of Induced W4A Expression on WAK Protein Reduction and Early Seedling Development.

**(A)** and **(B)** Immunocytochemical localization of WAK protein in DEX-treated ( $0.05 \mu\text{M}$  DEX in MS medium for 10 days) wild-type **(A)** and WAK4 antisense **(B)** plants. Sections of control plant **(A)** and W4A leaf **(B)** were probed with the WAK antibody. Antibody binding was detected with a fluorescein-conjugated secondary antibody. Green fluorescence indicating WAK protein and autofluorescence of chloroplasts (orange) in the mesophyll cells are superimposed. Bars =  $10 \mu\text{m}$ .

**(C)** and **(D)** Bright-field images of the sections in **(A)** and **(B)**, respectively. Bars =  $10 \mu\text{m}$ .

**(E)** DEX has a dramatic effect on W4A early seedling development. Seed from wild-type (WT) and WAK4 antisense transgenic (W4A) plants were grown on medium containing  $10 \mu\text{M}$  DEX. Photographs of representative seedlings were taken 20 days after germination.

cold treated, and plated on Petri dishes with MS medium containing 0.05  $\mu\text{M}$  DEX. At this concentration of DEX, W4A seedling development was retarded and the level of detectable WAK protein was reduced dramatically, as shown by protein gel blot analysis (see below). After 10 days, the treated seedlings were fixed and sectioned for immunolocalization. The WAK antibody was incubated with sections from DEX-treated wild-type and W4A plants. The antibody binding was detected by a fluorescein-conjugated secondary antibody. Figure 3A shows that WAK antibody bound to the surface of all cells of the wild-type leaves, which is consistent with previous data (He et al., 1996). Little antibody binding was detected in sections of DEX-treated W4A tissue (Figure 3B). The autofluorescence of chloroplasts in the mesophyll cells is shown in orange (Figures 3A and 3B). This experiment shows that WAK protein was essentially undetectable in DEX-induced W4A plants, which is consistent with the protein gel blot analysis.

Figure 3E shows that W4A seed placed on medium containing 10  $\mu\text{M}$  DEX can germinate but that they show developmental defects. Seed coat opening, initial hypocotyl elongation, and root radical elongation appeared normal. Further development, however, was arrested substantially. Cotyledons remained closed and yellow, and there was limited further root elongation (Figure 3E, W4A). DEX did not have any observable effect on control wild-type plant seedlings (Figure 3E, WT).

#### Correlation between DEX Concentration and Seedling Developmental Arrest

One advantage of the DEX-inducible system is that levels of gene expression can be correlated with the concentration of the inducer, DEX (Aoyama and Chua, 1997; McNellis et al., 1998). To analyze the specific dependence of lethality on the levels of WAK4 antisense expression, we tested the effect of different DEX concentrations on seed germination and early seedling development. WAK4 antisense transgenic seed were plated on growth medium containing a series of different DEX concentrations. As shown in Figure 4, the lowest concentration that had a visible effect on seedling development was 0.001  $\mu\text{M}$ . Between 0.001 and 1  $\mu\text{M}$ , there was a good correlation between the DEX concentration and developmental arrest. As the DEX concentration increased, root elongation and cotyledon opening were increasingly inhibited (enlarged images of individual seedlings in Figures 4D, 4F, 4H, and 4J). At 1  $\mu\text{M}$ , the inhibitory effect seemed saturated, because seedlings showed the same growth retardation phenotypes as did plants treated at higher DEX concentrations (5 and 10  $\mu\text{M}$ ; data not shown). DEX did not have any observable effects on seedlings of plants transformed with the pTA7002-*GUS* reporter gene (data not shown) or wild-type plants (Figures 4A, 4C, 4E, 4G, and 4I). *GUS* activities under these conditions also responded to different DEX concentrations (data not shown),

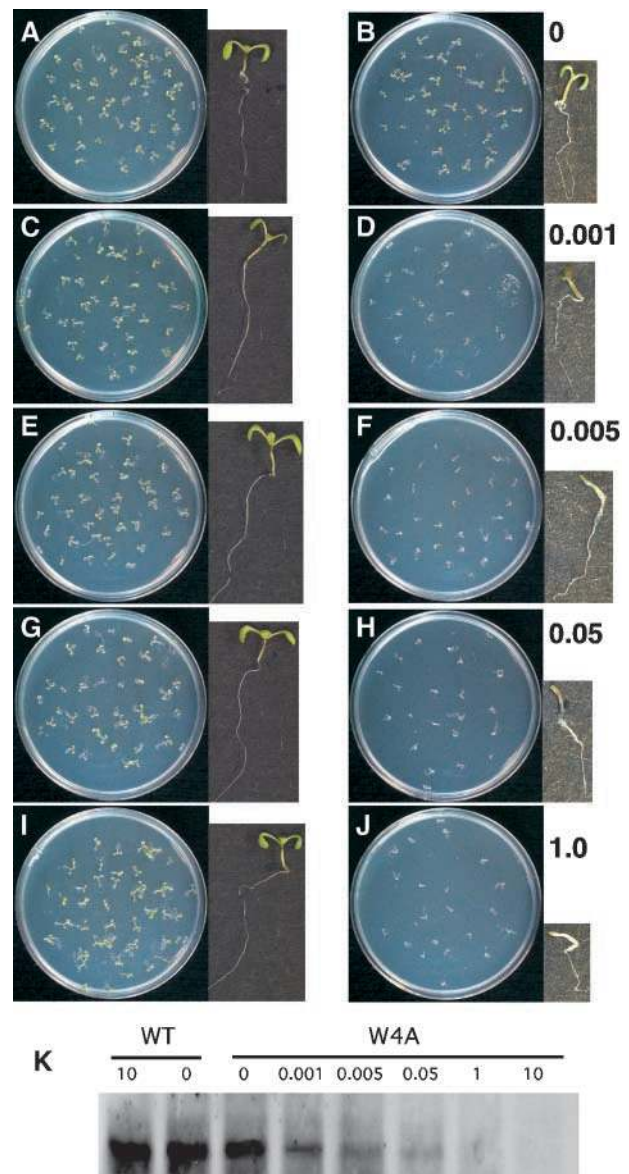


**Figure 4.** Dependence of Lethality of W4A Early Seedlings and WAK Protein Reduction on the Concentration of DEX.

(A) to (J) Correlation of W4A early seedlings and the concentration of DEX. Seed from wild-type plants ([A], [C], [E], [G], and [I]) and W4A plants ([B], [D], [F], [H], and [J]) were plated on MS medium containing 0  $\mu\text{M}$  ([A] and [B]), 0.001  $\mu\text{M}$  ([C] and [D]), 0.005  $\mu\text{M}$  ([E] and [F]), 0.05  $\mu\text{M}$  ([G] and [H]), or 1  $\mu\text{M}$  ([I] and [J]) DEX as indicated. An enlarged photograph of a representative seedling from each treatment is shown on the right. Photographs were taken 10 days after germination.

(K) Correlation of WAK protein reduction and DEX concentration. Equal amounts of total proteins extracted from either wild-type (WT) plants treated with 10 and 0  $\mu\text{M}$  DEX or W4A plants treated with 0, 0.001, 0.005, 0.05, 1, or 10  $\mu\text{M}$  DEX were fractionated by SDS-PAGE and analyzed by protein gel blotting using WAK antibody.

which is consistent with the reporter gene luciferase (Aoyama and Chua, 1997).

To confirm the correlation between the dosage of applied DEX and WAK protein levels, we extracted total protein from wild-type and W4A seedlings grown in medium at various DEX concentrations (Figures 4A to 4J). Equally loaded samples were fractionated using SDS-PAGE and analyzed by protein gel blotting. Figure 4K shows that WAK protein decreased as the amount of applied DEX increased. At DEX concentrations as low as 0.001  $\mu\text{M}$  in the growth medium, WAK protein in W4A seedlings decreased. When the DEX level reached 1  $\mu\text{M}$ , WAK protein levels became undetectable. These experiments suggest a close relationship between the severity of overall seedling developmental arrest and WAK protein levels.

### WAK4 Antisense Expression Impairs Growth and Development

DEX-induced WAK4 antisense expression had a profound effect on early seedling development. To further investigate the effect of WAK4 antisense expression in other developmental stages, we grew control and W4A plants in soil without DEX. At various developmental stages, plants were sprayed with 30  $\mu\text{M}$  DEX or a mock solution. Beginning at the six-leaf stage, two pots were selected from the wild-type and W4A plants and sprayed. Every 2 days, a new set of wild-type and W4A plants were selected and sprayed, and previously treated plants were retreated. The treatments were performed until plants bolted and flowered. As shown in Figure 5, the effects of WAK4 antisense expression were most prominent in seedlings in early developmental stages. Mature plants forming siliques showed little visible effects after treatment (Figure 5H) except for slightly shortened inflorescence stem tips. However, if the DEX treatment was started when W4A seedlings were at the six- to 10-leaf stage (Figures 5B to 5F), the effects were more dramatic. The overall seedling morphology of W4A plants (Figures 5B to 5F, [+]) was severely dwarfed compared with that of the control (Figures 5B to 5F, [-]). Leaves were small, and the lengths of inflorescence stems were reduced significantly.

Figure 6 shows a more detailed examination of these morphological alterations. In the presence of DEX, leaves grew vertically instead of horizontally (Figure 6A). Seedlings showed arrested growth and premature senescence during early development (Figure 6A). Interestingly, although abnormal, organs and tissues still could be established in later stage seedlings (Figures 5A to 5F and 6). Flowers were smaller and never opened (Figure 6B) but had complete organization of the organ layers (carpel, stamen, petal, and sepal). Siliques formed but were smaller and produced no fertile seed (Figures 6C and 6D). The lengths of inflorescence stems and floral pedicels were reduced dramatically (Figure 6D).

### WAK4 Antisense Expression Affects Cell Elongation

Plant growth and development rely on both cell division and cell elongation. The W4A dwarf morphology could be a result of disruptions in either cell division or cell elongation or both. Therefore, we compared both cell sizes and cell numbers from leaves, florescence stems, and silique pedicels in DEX-treated and untreated W4A plants. Tissues from W4A plants sprayed with DEX or a mock solution were fixed, and their epidermal images were obtained by scanning electron microscopy. As shown in Figure 7, leaf epidermal cells from DEX-treated plants were significantly smaller (Figure 7B) than those of untreated plants (Figure 7A). In addition to the size reduction, cell shapes in the DEX-treated W4A plants also were aberrant (Figure 7B). To accurately compare the cell numbers and sizes of the DEX-treated and untreated W4A plants, we sampled silique pedicels from both plants and fixed them for scanning electron microscopy. Pedicel expansion primarily occurs during flower formation and less so during silique development.

As shown in Table 1, the overall lengths of pedicels from DEX-treated plants were less than half the size of those from untreated plants. The average pavement epidermal cell number for both untreated and treated plants was essentially the same, 42 and 43 cells, respectively, along the pedicel length. However, the average length of a pavement epidermal cell in treated plants was <40% of the length of untreated plants (Table 1). These data indicate that cell elongation, not cell division, is affected by WAK4 antisense expression. Despite the striking size differences, epidermal differentiation appeared to be unaffected, as revealed by the overall cell numbers and the average distribution of stomata along the pedicels in both treated and untreated plants. The number of stomata along the pedicel remained unchanged, and the morphology of guard cells was unaffected by DEX treatment, as determined by scanning electron microscopy. Thus, the distribution pattern of stomata remained the same but the distances between stomata along the pedicel were reduced by slightly more than half. We conclude that the difference between treated and untreated plants is a function of the size of pavement epidermal cells separating stomata, not the number of cells.

Cell sizes also were analyzed in cells from inflorescence stems by using light microscopy. Epidermal peels of inflorescence stems from comparable parts of both DEX-treated (Figure 6D, [-]) and untreated (Figure 6D, [+]) W4A plants were obtained and stained with Lugol's solution and observed with a compound microscope. The sizes of cells of DEX-treated plants were found to be reduced by half (Figure 7D) compared with those of untreated plants (Figure 7C). Again, after counting stomata, we found that the distribution patterns of stomata remained the same (data not shown), which is consistent with the observations made with pedicels.

The inhibitory effect on cell elongation also was apparent when root lengths were measured. Wild-type and W4A seed were spotted to a medium that contained different concen-

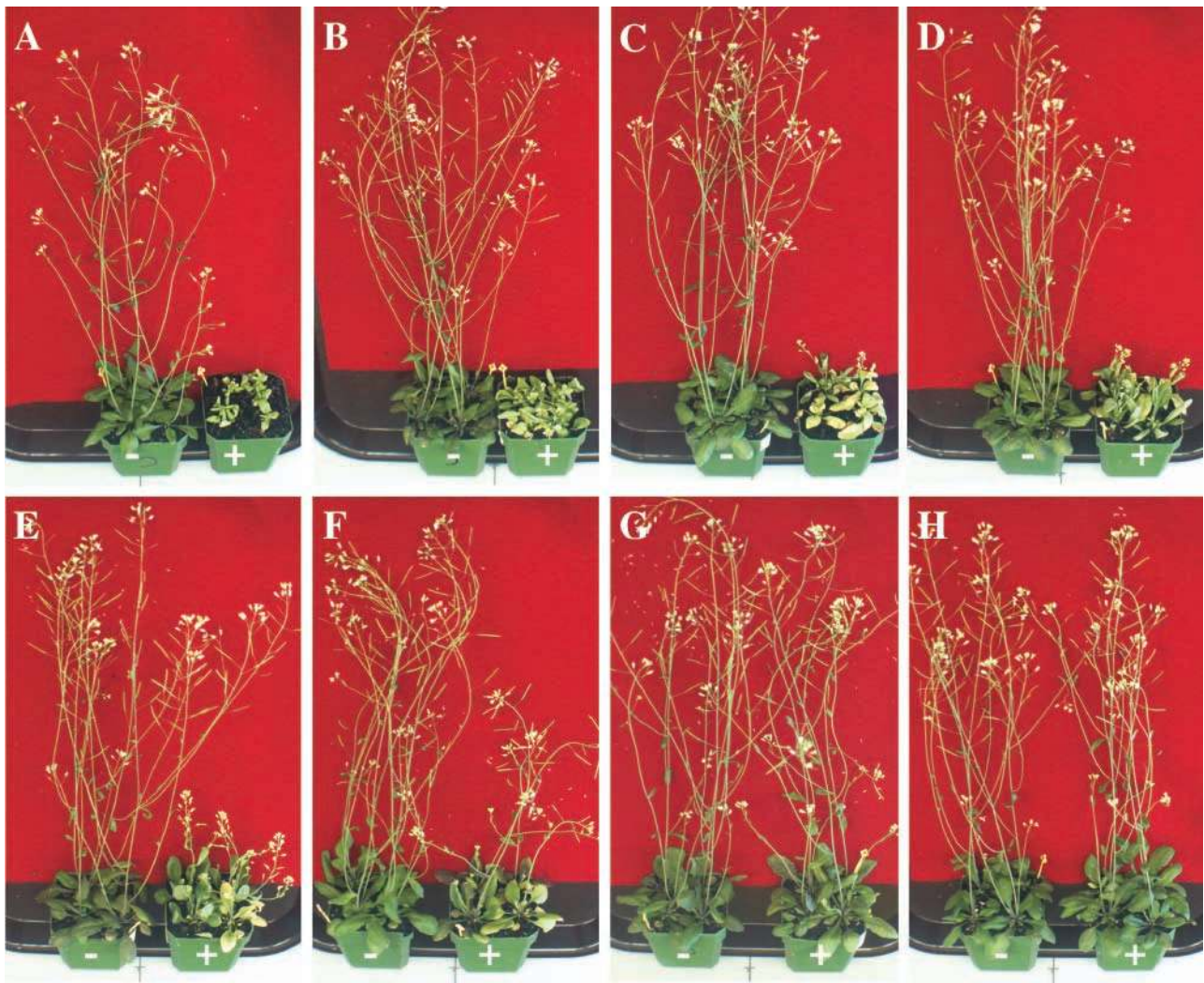


**Figure 5.** The Effects of W4A Expression on Development Are More Pronounced in Early Stages of Seedling Development and on Growing Parts of the Plants.

Starting at different stages (**[A]** to **[H]**), W4A transgenic plants were sprayed with either a mock solution (–) or 30  $\mu\text{M}$  DEX (+) every 48 hr. Starting stages: four leaf (**A**), six leaf (**B**), eight leaf (**C**), 10 leaf (**D**), 2 days after bolting (**E**), 4 days after bolting (**F**), 6 days after bolting (**G**), and 8 days after bolting (**H**). Photographs were taken 5 weeks after germination.

trations of DEX, as indicated in Figures 8A to 8D. For each treatment, wild-type and W4A seedlings were aligned on the same Petri dish. To conveniently measure the root length, we grew seedlings vertically on the surface of the MS agar medium and photographed them at 10 days after germination (Figures 8A to 8D). DEX had no effect on wild-type root elongation (Figures 8A to 8D, WT). Root elongation of W4A seedlings, however, was suppressed by DEX (Figures 8C and 8D, W4A). Root lengths of both wild-type and W4A seedlings were measured. There was no statistical difference in average root lengths between wild-type seedlings

grown at 0 and 0.05  $\mu\text{M}$  DEX or between W4A seedlings grown at 0 and 0.05  $\mu\text{M}$  DEX, as determined by a *t* test. However, at 0.05  $\mu\text{M}$  DEX, W4A plant shoot development was severely affected (Figure 8B, W4A). At 1.0  $\mu\text{M}$  DEX, the average root lengths of W4A seedlings were reduced by one-third, and at 10.0  $\mu\text{M}$ , root lengths were reduced by more than half compared with those of the wild type (Figure 8E). Interestingly, unlike shoot expansion, root elongation of W4A plants was never inhibited completely, even at 30  $\mu\text{M}$  DEX (data not shown). DEX-induced W4A root elongation appeared to be saturated in medium containing 10  $\mu\text{M}$  DEX.

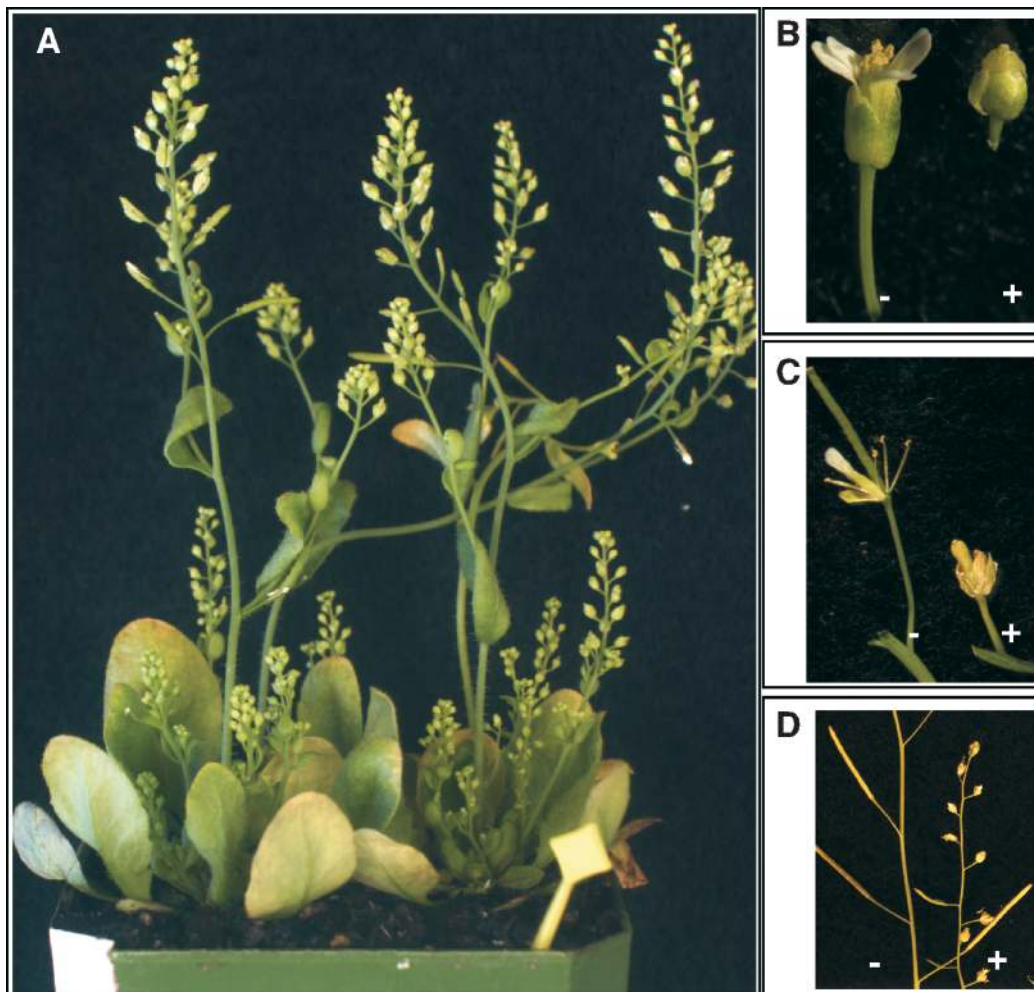


**Figure 6.** WAK4 Antisense Expression Results in Dwarf and Sterile Phenotypes.

**(A)** DEX-treated W4A plants appear to be dwarfed and have vertically grown leaves.

**(B)** DEX-treated W4A plants have smaller, unopened flowers (+) compared with those of the wild-type control (-).

**(C)** DEX-treated W4A plants have shortened siliques and pedicels (+) compared with those of the control wild-type plants (-). Siliques from the DEX-treated W4A plants (+) yield no viable seed.

**(D)** DEX-treated W4A plants yield shorter inflorescence stems and silique pedicels (+) compared with those of the wild-type control (-).

Compared with horizontally grown seedlings (Figure 4F), the vertically grown seedlings showed less severe responses when grown in medium containing identical DEX concentrations (Figure 8B; cf. Figure 4H). This likely is the result of the fact that the vertically grown roots may have less contact with the growth medium and thus may take up less DEX than roots grown horizontally.

Shoot development appeared more sensitive to DEX treatment than did root development. Figure 8E shows that roots composed ~20% of the total weight in both wild-type (DEX-treated or untreated) and W4A (untreated) seedlings. As the DEX concentration increased, shoot development

was severely repressed, whereas roots still gained a substantial amount of growth (Figures 8B to 8D). As a result, the percentage of root weight in total seedling weight increased (Figure 8E). When DEX concentration reached  $>1.0 \mu\text{M}$ , there was very limited shoot development and the root made up  $>80\%$  of the total seedling weight. At  $10.0 \mu\text{M}$  DEX, roots of W4A seedlings showed apparent abnormal development. Lateral root development was inhibited, and root hair elongation was reduced (Figure 8F, W4A). These results suggest that W4A expression affects cell elongation throughout the plant, although the sensitivity of organs varied.



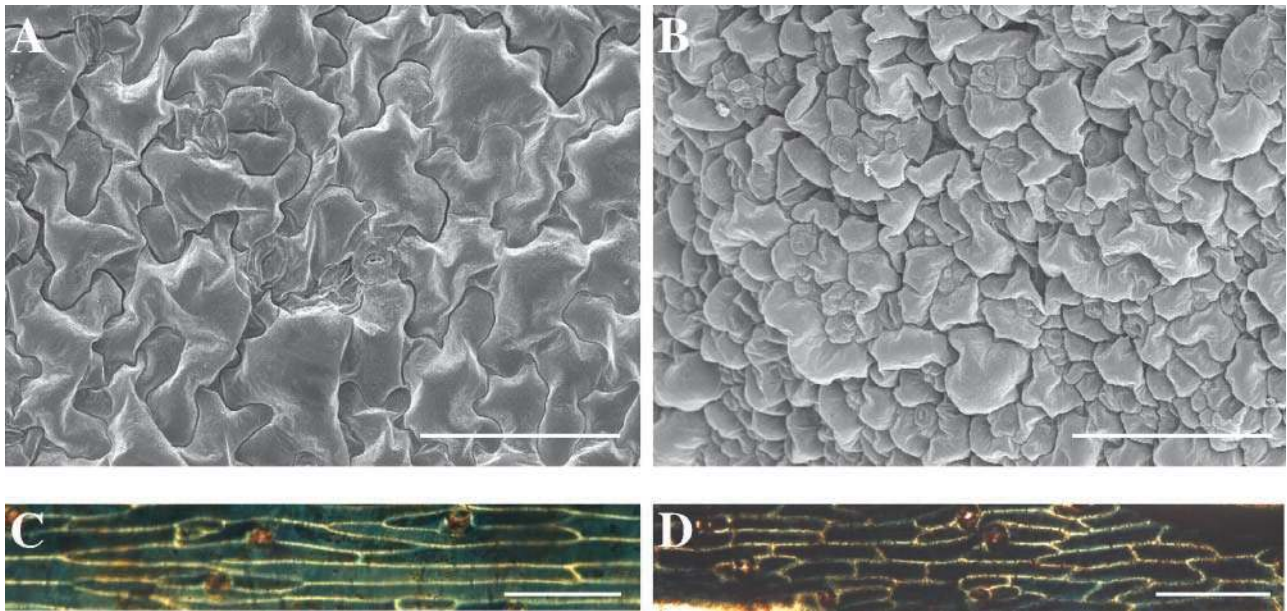


**Figure 7.** WAK4 Antisense Expression Affects Cell Elongation.

(A) and (B) Scanning electron micrographs of DEX-treated leaves from either a wild-type plant (A) or a W4A plant (B). Bars = 100  $\mu\text{m}$ . (C) and (D) Light microscope images of the epidermis of inflorescence stems from a DEX-treated wild-type plant (C) or a DEX-treated W4A plant (D). Hand peels of epidermis were stained with Lugol's solution and viewed with a compound microscope. Bars = 30  $\mu\text{m}$ .

## DISCUSSION

To determine the function of WAK4, we used the glucocorticoid-inducible system to control its antisense expression in Arabidopsis. We have shown that WAK4 antisense expression can effectively reduce WAK proteins, and the suppression of WAKs resulted in a series of dramatic pleiotropic effects on Arabidopsis growth and development. Our data strongly suggest a functional role for WAKs in cell elongation.

### Antisense Suppression of WAK Genes

In our study, when we induced antisense expression with DEX, we observed an increase of WAK4 mRNA and a decrease of WAK protein. These changes were confirmed in multiple W4A independent transgenic lines. Antisense expression has been used widely to manipulate endogenous gene expression, although its precise mechanism is not well known (Tang et al., 1999). It is generally believed that antisense RNA targets the endogenous gene transcript to form double-stranded RNA, which in turn triggers degradation of the transcript (Kennerdell and Carthew, 1998; Waterhouse et al., 1998). Although decreases of transcripts were reported in most studies, an increase was seen occasionally (D'Aoust et al., 1999). The mechanism of how WAK4 anti-

sense expression interferes with WAK gene function is not clear. The disappearance of all detectable WAK proteins suggests that W4A expression affects all WAK members. It is possible that the expression of the WAK4 antisense gene interferes directly with the transcription and/or translation of WAK4. This initial WAK4 gene suppression could result in the degradation of other WAK proteins. Alternatively, WAK4 antisense expression could interfere directly with the transcription of other WAK members. The latter possibility is unlikely because WAK4 antisense expression had little effect on the steady state levels of the transcripts of other WAK members, as shown by RNA gel blot analysis (Figure 1).

It is also possible that functional coordination exists

**Table 1.** Cell Length but Not Cell Number Is Affected by WAK4 Antisense Expression<sup>a</sup>

Parameter	Treatment	
	–DEX	+DEX
Pedicle length ( $\mu\text{m}$ )	5112 $\pm$ 766	2100 $\pm$ 470
Cell number/pedicle	42.3 $\pm$ 3.3	43.2 $\pm$ 3.8
Average cell length ( $\mu\text{m}$ )	120.9	48.6

<sup>a</sup>Data are means  $\pm$  SE of nine independent sample counts. Cell numbers were counted on scanning electron microscopic images as described in Methods.

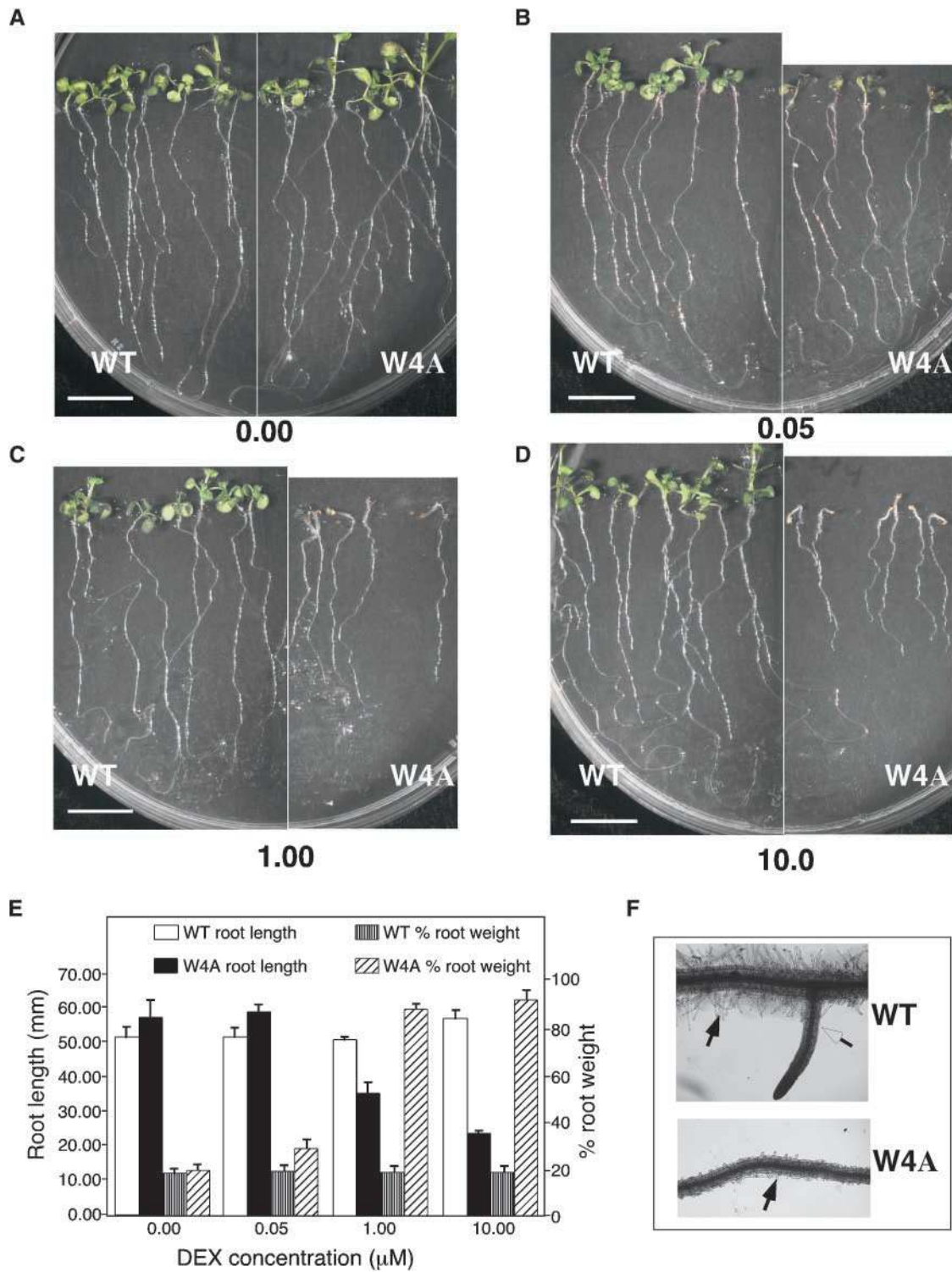


**Figure 8.** WAK4 Antisense Expression Affects Root Elongation.

(A) to (D) Relationship between DEX concentration and seedling development. Wild-type (WT) and W4A plants were germinated and grown vertically on MS medium containing various DEX concentrations (0.00  $\mu\text{M}$  [A], 0.05  $\mu\text{M}$  [B], 1.0  $\mu\text{M}$  [C], and 10.0  $\mu\text{M}$  [D]). For each treatment, wild-

between WAK4 and other WAK members. For example, different WAKs may work together as homodimers or heterodimers, and the destruction of one component may lead to the complete degradation of other partners. The well-characterized receptor-like protein kinase CLAVATA1 regulates both meristem and organ development in Arabidopsis. A related member, CLAVATA2, forms a heterodimer with CLAVATA1 and was found to be required for the normal accumulation of CLAVATA1 protein and its assembly into protein complexes (Jeong et al., 1999). Binding studies with bacterially expressed proteins indicate that WAKs bind to each other (Z.-H. He, unpublished data). Nevertheless, whether the physical binding exists in vivo and, if so, whether the stability of one WAK member relies on the presence of others remain to be determined by testing with specific antibodies to each WAK member.

Previous studies have shown that different WAK members are expressed in different organs and respond to different biotic and abiotic factors, suggesting that they may have distinct physiological functions (He et al., 1999). WAK4 was shown by RNA gel blot analysis to be expressed primarily in siliques (He et al., 1999). However, when a more sensitive detection method involving RT-PCR was used, WAK4 transcripts were found to be present in all organs tested (data not shown), including leaves. This finding suggests that WAK4 plays a functional role in most tissue types. It is expected therefore that the suppression of WAK4 may result in a variety of phenotypes. Pleiotropic effects of WAK4 antisense expression on growth and development are dramatic and can be observed at different stages, including early seedling development, inflorescence development, flower development, and seed formation.

In the glucocorticoid-inducible system, both the inducer, DEX, and the inducible system itself appear largely nontoxic to the plants and cause no adverse physiological effects (Aoyama and Chua, 1997; McNellis et al., 1998). However, it was reported recently that the glucocorticoid-inducible system could nonspecifically cause growth defects and induce defense-related genes (Kang et al., 1999). In that report, five of 21 transgenic lines carrying the empty transformation vector showed growth retardation (Kang et al., 1999). Therefore, we took extra precautions in analyzing our controls. Af-

ter initially using wild-type plants as controls, we repeated all of the experiments with transgenic plants that carried either the empty vector (pTA7002) or the *GUS* reporter gene (pTA7002-*GUS*) as controls. We observed a phenomenon similar to that reported by Kang et al. (1999) in two of 50 independent transgenic control lines; however, this kind of nonspecific effect caused by the glucocorticoid-inducible system can be screened out easily. It requires a much higher DEX concentration to achieve the growth defect phenotype. For example, a DEX concentration of 0.1  $\mu\text{M}$  was required to achieve the nonspecific phenotype (Kang et al., 1999), whereas 0.001  $\mu\text{M}$  was sufficient to have a dramatic effect on W4A seedlings (Figure 4D). Furthermore, the occurrence frequency of nonspecific defects is lower than that of the observed phenotypes in our W4A lines. In our studies, one-third of independent transgenic lines showed the same severe phenotypes. In addition, molecular analysis showed that WAKs were suppressed only in W4A transgenic plants, not in those plants whose growth and development were affected nonspecifically by the glucocorticoid-inducible system. The glucocorticoid-inducible system therefore still can be used as a reliable system to manipulate gene expression if appropriate controls are administered.

Aoyama and Chua (1997) reported that the lowest DEX concentration that had an inducible effect on the reporter gene luciferase in transgenic tobacco was 0.1  $\mu\text{M}$ . In the present study, however, the concentration of DEX that had an effect on transgenic Arabidopsis seedlings was much lower (0.001  $\mu\text{M}$ ; Figure 3D). At 0.001  $\mu\text{M}$  DEX, a decrease of WAK protein was readily observed (Figure 3K). This discrepancy may be the result of the slightly different experimental procedures used. The tobacco seedlings were grown in the absence of DEX and then transferred to medium containing DEX for 2 days before assay (Aoyama and Chua, 1997). In our study, Arabidopsis seedlings were placed on the medium with DEX, beginning at seed germination. Alternatively, Arabidopsis may be more sensitive to the inducible system than is tobacco. When the DEX-inducible system was used to study the lethal effect of the induced bacterial avirulence gene *avrRpt2* in Arabidopsis, the effective DEX concentration was found to be as low as 0.008  $\mu\text{M}$  (McNellis et al., 1998).

**Figure 8.** (continued).

type and W4A seed were germinated side by side on the same plate. A white line on each photograph separates the two groups. Photographs were taken 10 days after germination. Bars = 1 cm.

**(E)** Root length and weight measurements of DEX-treated and untreated wild-type and W4A plants. The roots of vertically grown plants (**(A)** to **(D)**) were measured using National Institutes of Health Image software. Values are averages of 10 independent measurements. Shoots and roots from these vertically grown seedlings were separated and weighed. The average percentage root weight in total seedling weight is shown. Error bars indicate  $\pm$ SE.

**(F)** WAK4 antisense expression suppresses lateral root development and root hair growth. Enlarged images of root segments of the seedlings in **(D)** are shown. Closed arrows indicate root hairs, and the open arrow indicates a lateral root.

### WAK4 Antisense Expression and Cell Elongation

Our analysis has indicated that the induced WAK4 antisense expression affects cell elongation but not cell division. DEX-treated W4A plants had small rosette leaves, condensed inflorescence stems, short siliques, unopened miniature flowers, and short primary roots. This phenotype was specific to the transgenic WAK4 antisense plants and was never observed in DEX-treated wild-type or transgenic empty vector plants. Measurements of total cells and total lengths in silique pedicels of DEX-treated control and W4A plants revealed that although the total cell number remained the same, cell length was reduced by >50%. Scanning electron microscopic examination of leaf epidermal cells from DEX-treated control and W4A plants showed that the sizes of leaf epidermal cells were reduced dramatically, consistent with the observation made in silique pedicels. The DEX-induced cell elongation inhibition was observed in other organs of W4A plants as well. For example, root elongation was inhibited dramatically by DEX treatment, and this inhibition appeared to be correlated closely with the amount of DEX applied.

Cell elongation involves turgor-driven expansion from wall component deposition or wall loosening. A number of internal and external factors, including environmental conditions (light and water), phytohormones (auxin, gibberellin, ethylene, and brassinosteroids), and developmental factors (cell type and cell age), can regulate either the wall-loosening properties or the way new wall components are deposited (Azpiroz et al., 1998; Jones, 1998; Bleecker and Kende, 2000; Sun, 2000). Exogenous application of auxin and gibberellin failed to rescue the W4A dwarf phenotype (data not shown), suggesting that cell expansion inhibition is unlikely to be the result of reduced levels of these phytohormones. A family of expansin proteins is known to be involved in loosening of noncovalent associations between cell wall polysaccharides, allowing turgor pressure to drive wall creep (Cosgrove, 1999). Expansin RNA levels were reduced dramatically when WAK expression was suppressed. This result suggests that WAKs can interact with a mechanism that regulates expansin expression. Although the connection between expansin and WAKs is unknown, the disappearance of WAKs may serve as a signal of cell wall disturbance and result in expansin decrease, thus resulting in the reduction of cell elongation. Whether and how WAK signal transduction pathways interact with expansins remain to be characterized.

### WAKs and Plant Development

Our data show that the repression of WAK-mediated cell expansion results in severe developmental retardation. The most severe phenotype is observed during early seedling development, when both shoot and root development are arrested (Figure 3E). If W4A plants are allowed to progress to later developmental stages at which all of the organs are

established before DEX treatment, their phenotypes vary and in general are limited to the actively growing portion of the organ. The various degrees of developmental arrest could be a reflection of the interruption of WAK functional roles at different developmental stages.

Scanning electron microscopic examination of epidermal cells in an expanding leaf of DEX-induced W4A plants revealed that not only were cell sizes reduced but cell shapes were altered as well. Although wild-type leaf epidermal cells showed a well-organized jigsaw organization, the pavement epidermal cells of W4A plants displayed a disorganized and rough morphology. Despite the disorganized appearance, however, all leaf epidermis cell types were present. Guard cells were still arranged in a pattern similar to that in wild-type plants. In all cases, DEX-induced WAK4 antisense expression never led to a phenotype that resulted in changes of organ numbers or identity.

Our data strongly suggest that shoot development is more sensitive to DEX treatment than is root development. Analyses of shoot and root weight in DEX-treated W4A seedlings suggest that although shoot growth was inhibited substantially at 1.0  $\mu$ M DEX, roots still gained a significant amount of growth (Figure 8E). As a result, root made up the majority of the seedling fresh weight. Morphologically, these DEX-treated W4A roots had shortened root hairs and little lateral root development (Figure 8F). The root hair initiation appeared to follow a normal pattern, but full expansion was lacking. The elongation of root hair depends on a process known as tip growth, in which cell elongation is limited to one region (the tip) (Benfey and Schiefelbein, 1994). In this mode of growth, secretory vesicles carrying new cell wall components and enzymes involved in cell elongation are directed to the tip of the growing cell. A number of genes have been identified in *Arabidopsis* that are required for the tip growth of root hair (Schiefelbein and Somerville, 1990; Schiefelbein et al., 1997). A few of them have been characterized recently (Pitts et al., 1998; Lee and Schiefelbein, 1999). It will be useful to determine whether and how WAKs interact with these components.

In conclusion, we have shown that the level of WAK expression can be controlled effectively by the induced expression of a WAK4 antisense gene. This provides evidence for the functional role of WAKs in cell expansion. Reduction of WAKs results in cell elongation inhibition and thus can affect development. Study of how WAKs control and interact with the cell elongation process will shed additional light on how WAKs function in regulating plant growth and development.

### METHODS

#### Plant Material

*Arabidopsis thaliana* ecotype Columbia wild-type and transgenic plants were grown as described previously (He et al., 1998). Plants

were grown either in soil or on Petri dishes with Murashige and Skoog (1962) (MS) medium. For plating, seed were surface sterilized by soaking for 20 min in sterile water followed by 5 min in 95% ethanol and then 5 min in 50% bleach. The seed were rinsed three times in sterile distilled water and then resuspended in 200  $\mu$ L of sterile water before being cold treated at 4°C for at least 2 days. For dexamethasone (DEX) treatment of soil-grown plants, aerial parts were treated with aerosol applications of 30  $\mu$ M DEX (Sigma).

### Construction of Transgenic Lines

The glucocorticoid-inducible transformation vector pTA7002 was kindly provided by Dr. Nam-Hai Chua (Rockefeller University, New York (Aoyama and Chua, 1997)). To generate the pTA7002 WAK4 antisense construct, the full-length WAK4 gene was amplified by polymerase chain reaction (PCR) from a WAK4 genomic clone (He et al., 1999). A *SpeI* site was introduced into the upstream primer (5'-AAG-AACTAGTTTGGAGAGAAAATAAATAAAG-3'), and a *XhoI* site was introduced into the downstream primer (5'-TTGGCTCGAGATATCAGC-GGCCTGCTTCAA-3'). The amplified 2.4-kb DNA fragment was digested by both *XhoI* and *SpeI* and ligated into the pTA7002 vector. The generated construct was further sequenced for confirmation and introduced into *Agrobacterium tumefaciens* (strain GV3101) cells for transformation (He et al., 1998). More than 23 independent lines were selected according to their hygromycin resistance. Homozygous transformants (T4) were confirmed by both segregation and PCR analysis. Backcrosses were performed to confirm that the transgenic lines carried one copy of the T-DNA. Two representative lines of WAK4 antisense gene were used for phenotypic analysis and molecular characterization. For controls, the empty vector or a pTA7002 construct carrying the  $\beta$ -glucuronidase (*GUS*) gene was used to generate transgenic plants in a similar manner.

### RNA Gel Blot and Protein Gel Blot Analyses

RNA was isolated as described previously (He et al., 1998). Fifteen micrograms of total RNA was fractionated and blotted onto a Hybond N<sup>+</sup> nylon membrane (Amersham Pharmacia Biotech). RNA gel blot hybridization was performed using a nonradioactive alkaline phosphatase (AP)-based technique according to the manufacturer's recommended protocol (Genisphere, Montvale, NJ). For the WAK2 probe, a gene-specific oligonucleotide (5'-ACAGATGCACAGTAG-GATGGTTGTGAAAGCTATGTGGTTTTACTCTGAC-3') was used to generate the 3DNA AP probe. For the WAK4 probe, the following 42-nucleotide DNA fragment was used: 5'-CCACTTCAAGGCCCTTAT-AGAATAGATCTCGTTCCACACAAC-3'. Briefly, these oligonucleotides were ligated to a 3DNA core molecule via a special 7-bp sequence overhang (5'-TTTTTCG-3'). The products generated were purified and hybridized to the RNA gel blots. After washing, the blots were further incubated with AP oligonucleotides that can hybridize specifically to the 3DNA core molecules. The presence of AP activities was detected by introducing a chemiluminescent substrate, CDP-Star (Amersham Pharmacia Biotech), and exposing the blot to x-ray film.

Protein extraction and protein gel blot analysis were performed as described previously (He et al., 1996). Equally loaded samples were fractionated on a 10% SDS-polyacrylamide gel and electroblotted onto a nitrocellulose membrane by using a semidry apparatus, as suggested by the manufacturer (Panther Semidry Blotter HEP-1; Owl Separation Systems, Portsmouth, NH). For time-course experi-

ments, WAK proteins were detected by using a rabbit polyclonal WAK antibody (1:5000) (He et al., 1996) and developed with enhanced chemiluminescence protein gel blot detection reagents (Amersham Pharmacia Biotech). For DEX dosage experiments, the WAK antibody was diluted 1:2750 and developed using a biotinylated secondary antibody and Duolux detection reagents (Vector Laboratories, Burlingame, CA).

### Immunolocalization

Arabidopsis seedlings were fixed in PBS (100 mM sodium phosphate, pH 7.5, and 100 mM NaCl) containing 4% paraformaldehyde, 0.5% Triton X-100, and 3% sucrose for 3 hr at 22°C. The fixed tissues were then washed in PBS-buffered 15% sucrose and quickly frozen in PolyFreeze (Polysciences, Warrington, PA) with liquid nitrogen. Twelve-micrometer-thick sections were cut on a cryostat (Leica, Northvale, NJ) at -20°C and transferred to Vectabond tissue adhesion reagent-coated slides (Vector Laboratories). Sections were blocked for 2 hr at 22°C with PBS containing 2% BSA and 1% goat serum. After a 2-hr incubation with WAK antibody (1:100 dilution in PBS), the sections were washed four times in PBS containing 0.1% Tween and once with PBS alone, followed by a 1-hr incubation with goat anti-rabbit IgG-fluorescein conjugate (Vector Laboratories). After four final washes with PBS containing 0.1% Tween and PBS alone, the slides were mounted in Vectashield (Vector Laboratories) and viewed with a Nikon Eclipse fluorescence microscope (Nikon, Melville, NY) with Fluor  $\times$ 100 objectives and imaged with an RT-SPOT camera with Simple PCI software (Diagnostic Instruments, Sterling Heights, MI). The presence of antibody binding was detected using an excitation light of 450 to 490 nm; the signal was captured in the green channel ( $\sim$ 515 nm). Chloroplasts give autofluorescence in the red range and are imaged in the red channel ( $\sim$ 615 nm). The pseudocolored green and red images were merged using SPOT software (Diagnostic Instruments). The figures were arranged using Adobe Photoshop version 5.0 (Adobe Systems, Mountain View, CA).

### Scanning Electron Microscopy and Cell Counting

Plant tissue was fixed in 37% formaldehyde, 5% acetic acid, and 50% ethanol under a gentle vacuum. Ethanol serial dehydration was performed at -20°C. Critical point drying was performed using an Autosamdri 814B critical point dryer (Toumisis Research, Rockville, MD), and gold-palladium sputter coating was performed with a Technics Hummer V (Technics, Alexandria, VA). Scanning electron microscopy images were made using a Philips XL 40 scanning electron microscope (Philips Electron Optics, Eindhoven, The Netherlands). Sections of inflorescence stem or silique pedicel were imaged by scanning electron microscopy, and epidermal cells were counted using Adobe Photoshop version 5.0.

### Light Microscopy

Whole plants were photographed with a cooled charge-coupled device color digital SPOT camera (Diagnostic Instruments) using a regular Nikon camera lens. The inflorescence stem epidermal tissues were peeled by hand and stained briefly in a Lugol's solution (iodine/potassium iodine; Sigma) and viewed with a microscope equipped with the SPOT digital camera. Root and whole seedling images were

obtained using a Zeiss Axiophot (Carl Zeiss, Thornwood, NY) dissecting scope with the SPOT camera.

### Root Length Measurements

Ten wild-type and W4A seed were germinated, spotted onto 0.8% plates at varying DEX concentrations, and placed vertically in a growth chamber at 22°C with 14 hr of light (200  $\mu$ E) to elicit normal root orientation. Fourteen-day-old seedlings were then imaged using a SPOT camera (Diagnostic Instruments), and the images were imported into NIH Image ppc v1.61 (National Institutes of Health, Bethesda, MD; <ftp://codon.nih.gov/pub/nih-image/>). A coimaged ruler was used to calibrate measurements. Distances were measured in micrometers by using the line tool option. Measurements were from the hypocotyl base to the root tips of primary roots. Each root was measured a minimum of three times. Data for each seed type at each treatment were combined to determine means and standard deviations.

### DEX Treatments

For the DEX concentration experiment, agar medium was prepared using 4.3 g of MS basal salt mixture (Sigma), 20 g of sucrose, 500 mg of Mes (Fisher Biotech, Fair Lawn, NJ), and 8 g of agar, and pH was adjusted to 5.7 with KOH. The medium was divided into nine Erlenmeyer flasks, autoclaved, and cooled to 60°C before adding 1  $\times$  vitamin and DEX (Sigma) at various concentrations: 0.001, 0.005, 0.05, 0.5, and 1.0  $\mu$ M. The medium was poured onto plates, and the plates were cooled and seeded with 20 to 25 seed per plate.

For the DEX treatment of plants at different developmental stages, wild-type and WAK4 antisense transgenic seed were plated on MS and MS/hygromycin agar media, respectively. Seedlings were transplanted to soil (four seedlings per pot) and grown to approximately the six-leaf stage. Beginning at the six-leaf stage, we selected two pots from the wild type and each W4A transgenic line. One of each was sprayed with a 30  $\mu$ M DEX solution containing 0.01% (w/v) Tween 20, and one was sprayed with a water solution containing 0.01% (w/v) Tween 20 (mock solution). Every succeeding 2 days, a new set of two pots from each line was selected and treated with DEX or water in a similar manner, and the previously treated plants were retreated. This procedure was performed every 2 days until a series of eight developmentally distinct initial spray periods existed. At the time that the eighth in the series was initiated, the plants were mature and flowering. The plants received continued applications every 2 days for 1 month after the eighth in the series was initiated.

### RNA Extraction and RT-PCR Analysis

Verification of WAK4 transcript accumulation was performed by reverse transcription (RT)-PCR. The indicated tissues (Figure 1B) were harvested and immediately frozen in liquid nitrogen. Total RNA was extracted using the RNeasy Plant Mini Kit (Qiagen, Valencia, CA) according to the manufacturer's instructions. RT-PCR analysis was performed on 0.1 to 1.0  $\mu$ g of total RNA (treated with DNase) by using the OneStep RT-PCR Kit (Qiagen). Reverse transcription was performed at 50°C for 30 min. Reaction mixtures were heated at 95°C for 15 min to activate HotStar Taq DNA Polymerase (Qiagen). PCR was performed for 35 cycles for WAK4 and for 30 cycles for actin under the following conditions: 94°C for 1 min, 58°C for 1 min, and 72°C for 1 min, followed by a final extension at 72°C for 10 min. Samples

were visualized on 3% agarose gels using a UV light transilluminator. To confirm the RT-PCR specificity for the WAK4 gene, we subcloned the generated RT-PCR product into a pGEM-T Easy Vector (Promega, Madison, WI) and subsequently sequenced it. The following primers were used: for WAK4, W4-220F (5'-GTTGTG-TGAACGAGAATCTATT-3') and W4-380R (5'-GAGAGTCAAATTACCTAGATTACT-3'); for actin (ACTIN2), ACTF (5'-TATTGAATTCCTTTGTGTGTTTGCAGC-3') and ACTR (5'-TGTTGGATCCCAACCATGACACCATG-3'); for expansin (At-EXP5), AtEXP-F (5'-CTCGCTCTCGTGGTTCATCTC-3') and AtEXP-R (5'-GGAGGACAAAAGTTAGTGGCAGTG-3').

### ACKNOWLEDGMENTS

We thank Dr. Joseph A. Verica (San Francisco State University) for helpful comments and discussion, Dr. Nam-Hai Chua (Rockefeller University) for the pTA7002 transformation vector, Dr. Bruce Kohorn (Duke University) for the WAK antibody, and Drs. Carmen Domingo and Jennifer Breckler (San Francisco State University) for help with the immunocytochemistry work. This work was supported by the National Institutes of Health MBRS-SCORE Program (Grant S06 GM52588), by National Institutes of Health Research Infrastructure in Minority Institutions Grant 5 P20 RR11805, and by National Science Foundation Grant MCB-9985135.

Received February 26, 2001; accepted April 11, 2001.

### REFERENCES

- Aoyama, T., and Chua, N.H. (1997). A glucocorticoid-mediated transcriptional induction system in transgenic plants. *Plant J.* **11**, 605–612.
- Appella, E., Robinson, E.A., Ullrich, S.J., Stoppelli, M.P., Corti, A., Cassani, G., and Blasi, F. (1987). The receptor-binding sequence of urokinase: A biological function for the growth-factor module of proteases. *J. Biol. Chem.* **262**, 4437–4440.
- Azpiroz, R., Wu, Y., LoCascio, J.C., and Feldmann, K.A. (1998). An Arabidopsis brassinosteroid-dependent mutant is blocked in cell elongation. *Plant Cell* **10**, 219–230.
- Baskin, T.I., Wilson, J.E., Cork, A., and Williamson, R.E. (1994). Morphology and microtubule organization in *Arabidopsis* roots exposed to oryzalin or taxol. *Plant Cell Physiol.* **35**, 935–942.
- Bechtold, N., Ellis, J., and Pelletier, G. (1993). *In planta Agrobacterium* mediated gene transfer by infiltration of adult *Arabidopsis* plants. *C. R. Acad. Sci.* **316**, 1194–1199.
- Benfey, P.N., and Schiefelbein, J.W. (1994). Getting to the root of plant development: The genetics of *Arabidopsis* root formation. *Trends Genet.* **10**, 84–88.
- Bleecker, A.B., and Kende, H. (2000). ETHYLENE: A gaseous signal molecule in plants. *Annu. Rev. Cell Dev. Biol.* **16**, 1–18.
- Braam, J. (1999). If walls could talk. *Curr. Opin. Plant Biol.* **2**, 521–524.
- Carpita, N.C., and Gibeaut, D.M. (1993). Structural models of pri-

- mary cell walls in flowering plants: Consistency of molecular structure with the physical properties of the walls during growth. *Plant J.* **3**, 1–30.
- Carpita, N., McCann, M., and Griffing, L.R.** (1996). The plant extracellular matrix: News from the cell's frontier. *Plant Cell* **8**, 1451–1463.
- Cosgrove, D.J.** (1997). Relaxation in a high-stress environment: The molecular bases of extensible cell walls and cell enlargement. *Plant Cell* **9**, 1031–1041.
- Cosgrove, D.J.** (1999). Enzymes and other agents that enhance cell wall extensibility. *Annu. Rev. Plant Physiol. Plant Mol. Biol.* **50**, 391–417.
- D'Aoust, M.-A., Yelle, S., and Nguyen-Quoc, B.** (1999). Antisense inhibition of tomato fruit sucrose synthase decreases fruit setting and the sucrose unloading capacity of young fruit. *Plant Cell* **11**, 2407–2418.
- Fleming, A.J., McQueen-Mason, S., Mandel, T., and Kuhlemeier, C.** (1997). Induction of leaf primordia by the cell wall protein expansin. *Science* **276**, 1415–1418.
- He, Z.-H., Cheeseman, I., He, D., and Kohorn, B.D.** (1999). A cluster of five cell wall-associated receptor kinase genes, WAK1–5, are expressed in specific organs of *Arabidopsis*. *Plant Mol. Biol.* **39**, 1189–1196.
- He, Z.-H., Fujiki, M., and Kohorn, B.D.** (1996). A cell wall-associated receptor-like protein kinase. *J. Biol. Chem.* **271**, 19789–19793.
- He, Z.-H., He, D., and Kohorn, B.D.** (1998). Requirement for the induced expression of a cell wall associated receptor kinase for survival during the pathogen response. *Plant J.* **14**, 55–63.
- Jeong, S., Trotochaud, A.E., and Clark, S.E.** (1999). The *Arabidopsis* *CLAVATA2* gene encodes a receptor-like protein required for the stability of the *CLAVATA1* receptor-like kinase. *Plant Cell* **11**, 1925–1934.
- Jones, A.M.** (1998). Auxin transport: Down and out and up again. *Science* **282**, 2201–2203.
- Kang, H.G., Fang, Y., and Singh, K.B.** (1999). A glucocorticoid-inducible transcription system causes severe growth defects in *Arabidopsis* and induces defense-related genes. *Plant J.* **20**, 127–133.
- Kennerdell, J.R., and Carthew, R.W.** (1998). Use of dsRNA-mediated genetic interference to demonstrate that *frizzled* and *frizzled 2* act in the wingless pathway. *Cell* **95**, 1017–1026.
- Kim, G.T., Tsukaya, H., Saito, Y., and Uchimiya, H.** (1999). Changes in the shapes of leaves and flowers upon overexpression of cytochrome P450 in *Arabidopsis*. *Proc. Natl. Acad. Sci. USA* **96**, 9433–9437.
- Kohorn, B.D.** (2000). Plasma membrane-cell wall contacts. *Plant Physiol.* **124**, 31–38.
- Lee, M.M., and Schiefelbein, J.** (1999). WEREWOLF, a MYB-related protein in *Arabidopsis*, is a position-dependent regulator of epidermal cell patterning. *Cell* **99**, 473–483.
- McCarty, D.R., and Chory, J.** (2000). Conservation and innovation in plant signaling pathways. *Cell* **103**, 201–209.
- McNellis, T.W., Mudgett, M.B., Li, K., Aoyama, T., Horvath, D., Chua, N.H., and Staskawicz, B.J.** (1998). Glucocorticoid-inducible expression of a bacterial avirulence gene in transgenic *Arabidopsis* induces hypersensitive cell death. *Plant J.* **14**, 247–257.
- Murashige, T., and Skoog, F.** (1962). A revised medium for rapid growth and bioassays with tobacco tissue cultures. *Physiol. Plant.* **15**, 473–497.
- Pitts, R.J., Cernac, A., and Estelle, M.** (1998). Auxin and ethylene promote root hair elongation in *Arabidopsis*. *Plant J.* **16**, 553–560.
- Pont-Lezica, R.F., McNally, J.G., and Pickard, B.G.** (1993). Wall-to-membrane linkers in onion epidermis: Some hypotheses. *Plant Cell Environ.* **16**, 111–123.
- Rebay, I., Fleming, R.J., Fehon, R.G., Cherbas, L., Cherbas, P., and Artavanis-Tsakonas, S.** (1991). Specific EGF repeats of Notch mediate interactions with Delta and Serrate: Implications for Notch as a multifunctional receptor. *Cell* **67**, 687–699.
- Roberts, K.** (1994). The plant extracellular matrix: In a new expansive mood. *Curr. Opin. Cell Biol.* **6**, 688–694.
- Schiefelbein, J.W., and Somerville, C.** (1990). Genetic control of root hair development in *Arabidopsis thaliana*. *Plant Cell* **2**, 235–243.
- Schiefelbein, J.W., Masucci, J.D., and Wang, H.** (1997). Building a root: The control of patterning and morphogenesis during root development. *Plant Cell* **9**, 1089–1098.
- Stenberg, Y., Muranyi, A., Steen, C., Thulin, E., Drakenberg, T., and Stenflo, J.** (1999). EGF-like module pair 3–4 in vitamin K-dependent protein S: Modulation of calcium affinity of module 4 by module 3, and interaction with factor X. *J. Mol. Biol.* **293**, 653–665.
- Sun T.-p.** (2000). Gibberellin signal transduction. *Curr. Opin. Plant Biol.* **3**, 374–380.
- Tang, G.Q., Luscher, M., and Sturm, A.** (1999). Antisense repression of vacuolar and cell wall invertase in transgenic carrot alters early plant development and sucrose partitioning. *Plant Cell* **11**, 177–189.
- Torii, K.U.** (2000). Receptor kinase activation and signal transduction in plants: An emerging picture. *Curr. Opin. Plant Biol.* **3**, 361–367.
- Waterhouse, P.M., Graham, M.W., and Wang, M.B.** (1998). Virus resistance and gene silencing in plants can be induced by simultaneous expression of sense and antisense RNA. *Proc. Natl. Acad. Sci. USA* **95**, 13959–13964.
- Wyatt, S.E., and Carpita, N.C.** (1993). The plant cytoskeleton-cell wall continuum. *Trends Cell Biol.* **3**, 413–417.
- Wymer, C., and Lloyd, C.** (1996). Dynamic microtubules: Implications for cell wall patterns. *Trends Plant Sci.* **1**, 222–228.
- Yoshizumi, T., Nagata, N., Shimada, H., and Matsui, M.** (1999). An *Arabidopsis* cell cycle-dependent kinase-related gene, *CDC2b*, plays a role in regulating seedling growth in darkness. *Plant Cell* **11**, 1883–1896.
- Zhu, J.K., Shi, J., Singh, U., Wyatt, S.E., Bressan, R.A., Hasegawa, P.M., and Carpita, N.C.** (1993). Enrichment of vitronectin- and fibronectin-like proteins in NaCl-adapted plant cells and evidence for their involvement in plasma membrane-cell wall adhesion. *Plant J.* **3**, 637–648.